

Damage and Repair of Skeletal Muscle Microstructure after Basketball Exercise and Protein Nutrition Supplement Based on CT Images

Sahil Kavita*

University of Rochester, America

**corresponding author*

Keywords: CT Image Analysis, Basketball Exercise, Eccentric Exercise, Skeletal Muscle Serum, Skeletal Muscle Microstructure

Abstract: There are many types of skeletal muscle injury, which can be divided into laceration, blunt contusion, strain, shear injury, etc., which are blunt contusion and strain. The occurrence of injury is mainly dependent on the stress condition of the muscle, the texture and nutritional state of the muscle, and the correct training method and the balance of strength are also the key factors. To observe the injury and repair of skeletal muscle microstructure after basketball exercise and the intervention effect of protein nutrition supplement. CT functional imaging (computed tomography functional imaging) has the advantages of simple operation, reproducible and safety, where perfusion imaging evaluates tissue perfusion at capillary levels and is more closely related to tissue metabolism; energy spectroscopy imaging can accurately measure iodine concentration in the tissue and achieve quantitative analysis of lesions. At present, CT functional imaging has been widely used in brain, heart, lung, kidney, liver and other organs, which plays an important guiding role in ischemia-reperfusion changes and qualitative diagnosis of tumor and evaluation of efficacy after chemotherapy and chemotherapy. The rats centrifugal motion model to simulate the basketball sports, the rats were divided into control group, eccentric exercise group immediately, 24h, 48h group, eccentric exercise groups other than the control group the adaptability of the centrifugal training for 6 weeks, respectively observation campaign group rat skeletal muscle after eccentric exercise serum CK-MM, Calpain, gastrocnemius Titin and Nebulin protein expression. Compared with the control group, the activity content of CK-MM in the serum of rats after exercise was significantly increased, reaching the peak 24 hours later, and showing a downward trend at the 48h stage. Titin protein content is significantly reduced after the movement of the gastrocnemius muscle, calf Nebulin in cracking protein supplement after take effect 24 hours a day. The content of β -glucosidase in skeletal muscle increased sharply immediately after exercise and gradually decreased until 48 hours after exercise. The G6PDH content of skeletal muscle also increased significantly after exercise, reaching its peak at 24h after exercise. After strenuous exercise, the membrane permeability of the body is increased under heavy

load, leading to protein degradation immediately after exercise, and exercise-induced ischemia-reperfusion is an important reason to induce skeletal muscle microstructure damage.

1. Introduction

The competition of competitive sports at home and abroad is becoming more and more intense. Athletes must develop their potential to the greatest extent within the range of their physical endurance, so that they have the quality conditions to impact the limit. However, if athletes only rely on hard training in the process of training, it is difficult to achieve better performance on the top platform. Instead, scientific training should be combined with reasonable nutrition supplements to improve their training efficiency and enhance their extreme sports ability. Improper training methods and neglect of nutritional supplements are easy to cause sports skeletal muscle damage. This kind of unscientific training, which is eager for quick success and instant benefits, gradually highlights the contradiction between the increasing exercise load and the endurance capacity of the body skeletal muscle. Therefore, to explore the mechanism of the structural and physical changes of exercisable skeletal muscle and propose reasonable nutritional supplements to reduce the incidence of structural injury has always been a research hotspot in sports medicine.

Sports injury usually occurs after high-intensity or long-term exercise, and is a pathological mechanism of skeletal muscle fiber microstructure changes, mainly manifested as abnormal myocyte metabolic function, ultrastructural damage, and electromyographic index changes or functional decline [1]. Skeletal muscle microstructures have delayed characteristics and are associated with symptoms of muscle soreness [2]. Different from muscle contusion in sports traumatology, skeletal muscle fiber micro-injury is continuously aggravated within a period of time after exercise, generally reaching the peak of injury 48 hours after exercise, and the symptoms will gradually relieve and disappear after several days [3-4].

Regardless of the athletic level of athletes, high-intensity athletic training or long-term endurance training will cause the decline of skeletal muscle contraction function, body fatigue and the injury of muscle microstructure. Delayed onset muscle soreness (DOMS) is an inevitable painful experience for athletes in their career [5]. From the beginning of last century to the near stage, there have been many reports on the indicator detection and occurrence mechanism of DOMS, mainly focusing on free radical damage, acute inflammatory reaction, muscle spasm, accumulation of metabolites and mechanical damage hypothesis [6-7]. Numerous studies have shown that delayed muscle soreness is closely related to the occurrence and development of hypoxia regulation (EIMD), and DOMS is believed to be a series of subjective changes caused by EIMD [8]. Therefore, the study on EIMD is helpful to prevent, mitigate and avoid DOMS. At present, there are also relatively many reports on EIMD, but there are still relatively few studies on its protective measures, detection methods and pathogenesis, and no direct comparative studies on ischemia-reperfusion injury and skeletal muscle EIMD [9-10]. Some studies have suggested that IL-6 may be associated with sportive skeletal muscle microinjury, but whether it can be used as a detection indicator for EIMD has not been determined [11]. Serum creatine kinase (CK) is generally considered as a sensitive indicator for evaluating muscle injury, but CK is a stress enzyme, and the rules of change are inconsistent with those of muscle injury, so there is a big difference [12-13]. Some studies have

reported that serum skeletal muscle troponin (STNI) is a landmark indicator of muscle injury, but this detection method is not practical because of the high reagent cost [14-15]. Therefore, this study aims to study the occurrence of skeletal muscle microdamage and repair process under nutritional intervention from the perspective of morphology and metabolism, so as to provide experimental support for the development of new nutritional supplements.

Skeletal muscle injury self-repair process divided into three stage injury muscle injury hematoma, muscle fiber membrane damage, damaged muscle degeneration, degeneration, neutrophil infiltration, macrophages cruise to the damage phagocytic necrotic tissue repair period is located around the damage muscle in the stationary period, by growth factors and damage muscle release signal stimulation activation, swim to the damage hyperplasia, fusion, form striatal muscle. Fibroblasts invade the gap and produce the extracellular matrix to restore the connected tissue architecture, along with tissue revascularization. If the range of damage is too large, a large number of dense connective tissue formation, will reduce the mass tissue shaping period regeneration skeletal muscle maturation, paralysis mark tissue mechanization. Therefore, generally blunt contusion skeletal muscle often does not fully return to an undamaged functional state after natural healing. The rats centrifugal motion model to simulate the basketball sports, the rats were divided into control group, eccentric exercise group immediately, 24h, 48h group, eccentric exercise groups other than the control group the adaptability of the centrifugal training for 6 weeks, respectively observation campaign group rat skeletal muscle after eccentric exercise serum CK-MM, CalpainI, gastrocnemius Titin and Nebulin protein expression. Compared with the control group, the activity content of CK-MM in the serum of rats after exercise was significantly increased, reaching the peak 24 hours later, and showing a downward trend at the 48h stage. Titin protein content is significantly reduced after the movement of the gastrocnemius muscle, calf Nebulin in cracking protein supplement after take effect 24 hours a day [16-17].

2. Research Overview

2.1. CT Image Analysis Technology

(1) The structure and principle of CT equipment

A complete CT system is mainly composed of a scanning part, high-speed computer hardware, a complete image reconstruction, display, recording and post-processing system, and an operation control part. The CT instrument can be divided into three parts: 1) The scanning part composed of X-ray tube, detector and scanning frame; 2) The computer system that stores and calculates the information and data collected by the scan; 3) After processing and reconstruction The image display and storage system of the image display and storage is shown in Figure 1, the working principle of CT and the CT scan image of the mouse shown in Figure 2.

Different tissues and organs in the human body have different absorption coefficients of X-rays. CT technology uses this principle for imaging, that is, the attenuation characteristics of X-rays after passing through the human body are used for imaging, and the attenuation law of X-ray index is followed:

$$I_{out} = I_{in}e^{-\mu d} \quad (1)$$

In formula (1), μ : the absorption coefficient of the object to X-rays, which is related to the density of the object; d : the thickness of the object; I_{in} : the incident intensity of X-rays; I_{out} : the intensity of the X-rays attenuated by the object.

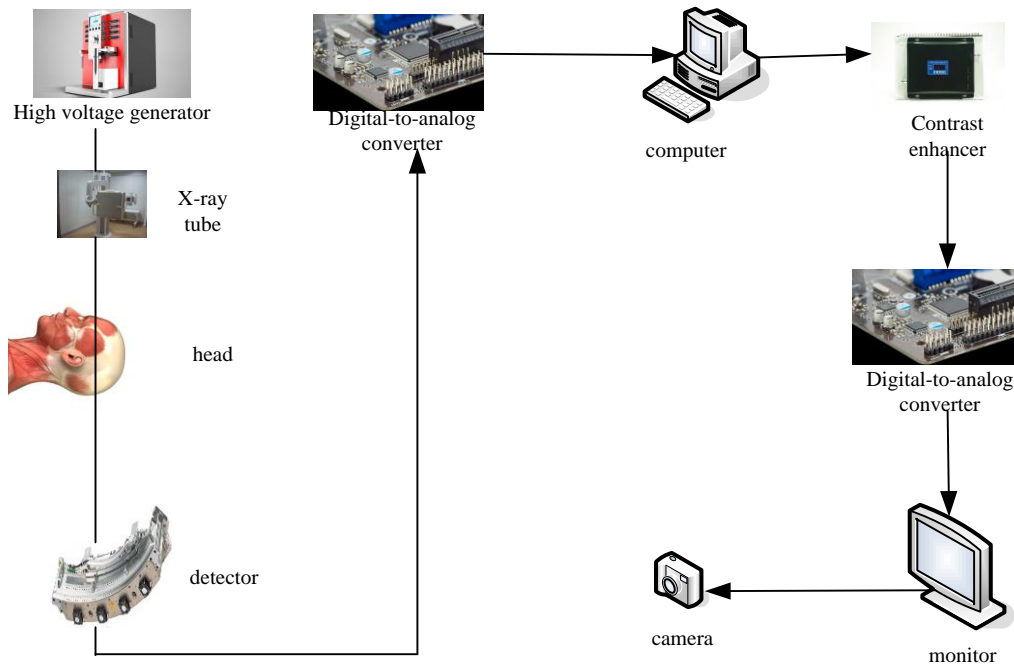


Figure 1. The working principle of CT

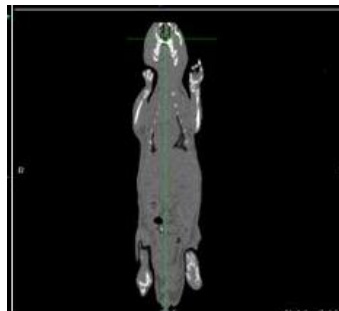


Figure 2. CT scan image of a mouse

At present, many technical means can be used to evaluate skeletal muscle microcirculation, such as perfusion fluorescence analysis, hyperspectroscopic imaging, nuclear diagnostic imaging, laser Doppler, etc. In addition to the above indirect quantitative analysis of microcirculation, autofluorescence confocal microscopy can directly observe the changes in tissue microcirculation, but the above technology is still in the research stage, and autofluorescence confocal microscopy is invasive examination and has not been fully adapted to clinical practice. However, CT functional imaging technology is a noninvasive technique that can assess tissue perfusion from capillary levels, and is more closely related to tissue metabolism.

When X-rays pass through a series of tissues and organs with different absorption coefficients but the same thickness, the relationship between the output intensity and the incident intensity is as follows:

$$I_{put} = I_{in} e^{-\mu_1 d} \bullet e^{-\mu_2 d} \bullet e^{-\mu_3 d} \bullet \bullet \bullet \bullet e^{-\mu_n d} \quad (2)$$

which is:

$$I_{out} = I_{in} e^{-\int nd} \quad (3)$$

SC plays a pivotal role in the repair of skeletal muscle injury. SC is long-standing as a muscle precursor cell (mpc) in mature skeletal muscle, located between the substrate and each myofiber cytosolic membrane. Normally SC is in quiescent phase but has characteristic of embryonic muscle cells. SC is activated in response to muscle injury, and in the case of intact basal lamina, express muscle regulators (MuscleRegulateFactor, MRF) such as MyoD, Myf5, then proliferate, differentiate into multinucleated myotubes, synthesize some important functional proteins of the muscle and eventually fuse into myofibers.

The CT image is a reconstructed image, and the imaging process is shown in Figure 1: A certain part of the human body is scanned with a certain thickness, and the attenuated X-ray signal is received by the detector, and after it is converted into visible light, it is converted from photoelectric to electrical signal. Then it is converted to digital by analog/digital converter and input into computer; the processing of image formation divides the selected layer into several rectangular parallelepipeds of the same volume, called voxels; the scanned information is calculated to obtain the X-ray attenuation of each voxel. The absorption coefficients are then arranged into a matrix, that is, a digital matrix; each number is converted into small squares with different gray levels from black to white through a digital/analog converter, that is, pixels, which are arranged in a matrix, that is Compose the CT image, as shown in Figure 3, the repair process of human skeletal muscle microstructure after injury.

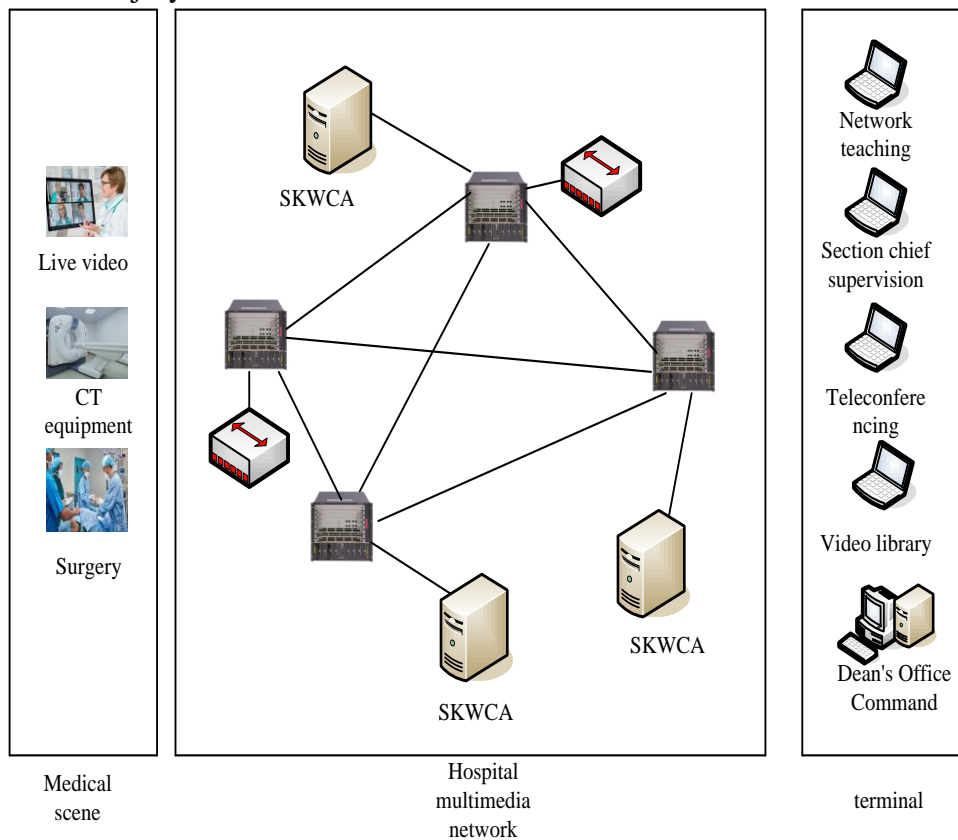


Figure 3. The treatment and repair process of human skeletal muscle microstructure after injury

2.2. Protein Digestion and Absorption

Protein is a large molecule with high specificity. It is difficult to be fully digested in the stomach, so it is not easy to be absorbed and utilized. It must be broken down into small molecules in the digestive tract before it can be absorbed and utilized by the body. Protein in the small intestine not only has the digestive function of the small intestinal mucosal cells themselves, but also secretes digestive fluid to assist digestion, therefore, the main site of protein digestion and absorption is the small intestine.

The proteolytic enzymes in the small bowel are dipeptidase, Aminopeptidase APN and Enterokinase. The enzymes involved in protein digestion in pancreatic juice were procarboxypeptidase A&B, Proelastase, chymotrypsinogen and Trypsinogen. Carboxyl peptidase and amino peptidase are from the outer end of the peptide chain respectively, and each hydrolysis can produce the next amino acid, while elastin, chymotrypsinogen and trypsinogen are all endopeptidase, which can hydrolyze some peptide bonds inside the peptide chain, so they are called exopeptidase.

In recent years, helical CT has been continuously, and the spatial resolution and scanning speed of scanning Z axis have been significantly improved. At the same time, with the emergence of the core technology of the instantaneous dual kVp, the energy spectrum CT has also been widely used. CT functional imaging can not only show tissue or organ morphological information, but also noninvasively non-invasive, quantitative or semi-quantitative multiple parameters to assess the hemodynamic status of tissue or organs and their functional information, more closely related to tissue metabolism.

There is also a larger molecule peptide absorption form in small intestinal epithelial cells, which belongs to the intercellular micropore absorption form. It can be induced by the traction of lysozyme or the stimulation of lysozyme, or by the vacancy left by shedding or endocytosis in epithelial cells, resulting in the non-selective absorption of the peptide. Therefore, peptide absorption is different from other single-chain absorption. It not only transmits the structure information of the peptide to the host, reflects different biological activities through the diversity of amino acid composition sequence, but also provides nitrogen source for the body. Therefore, although the nutritional significance of peptides may not be important, they are important for the expression of biodiversity in the body.

2.3. Determination of Protein Nutritional Value, Exercise and Protein Metabolism

(1) Determination of the nutritional value of protein

The nutritional value of food protein is evaluated from the perspective of quality, that is, the content and mode of essential amino acids in food protein, and from the perspective of quantity, that is, the amount of protein in food. In addition, the body itself to protein digestion, utilization rate is also an important factor of protein nutritional value. Compared with food protein, the essential amino acid protein and its ratio are in a pattern with the essential amino acid demand of human body. The more essential nutrients there are in food protein, the more balanced the amino acid is and the higher the utilization rate is. In the classical theory of nutrition, the bucket rule holds that the nutritional value of food protein depends on the minimum amount of essential amino acids. After the birth of the nutritive peptide theory, the bucket rule has been seriously challenged. According to the nutritive peptide theory, the utilization rate of protein is summarized as the degree to which food protein is digested and absorbed in the stomach, and the indexes to measure these degrees include true digestibility and apparent digestibility. At the level of biological indicators, the

cost of protein production, protein efficiency ratio, protein net utilization rate and protein retention rate must all depend on microbiological assay.

(2) Exercise and Protein Metabolism

Basketball was invented in 1891 by American James Naismith. At the time, he taught at the YMCA International Training School in Springfield, Massachusetts. Because the local is rich in peaches, children here very like to play the game of putting the ball into the peach basket. This inspired him from it and developed other ball such as football and hockey and created basketball games. The initial basketball game was relatively simple, with no limit on venue size or the number of participants. The players were divided into equal teams, standing at both ends of the pitch. After the referee threw the ball at the center, the players immediately rushed into the pitch and tried to throw it into the other side's basket. Because the peach basket is bottom, the ball remains in the basket, people must board a special ladder to remove the ball from the basket. With the continuous improvement of field facilities, the basket cancelled the bottom and switched to iron circles instead of peach baskets, made of wooden boards instead of wire block, added the center line, center circle and free throw line, and the game began with midfield jumps. At the same time, the game players are usually changed to five players per team, starting to have the guard, guard, center, forward, left behind and other positions. In addition, Naismith formulated a very imperfect competition rule with 13 terms, which were not allowed to take the ball, hug, push, trip, hit, etc. This greatly improved the fun of basketball games and attracted more people to the game, quickly enabling the popularity of basketball throughout the United States.

The research on protein metabolism of human body by sports training and physical activity has not been fully interpreted after nearly a century of research, and the opinions on supplementation of protein and amino acids by athletes have not yet formed a consensus. Therefore, various basic researches have not yet reached a consensus on protein metabolism of the body. There is no uniform standard for the optimal protein intake of athletes. On the one hand, this is caused by a variety of complex factors. On the other hand, unscientific nutritional supplements and unreasonable dietary structure of athletes also account for the main reasons. There are still technical difficulties in quantifying protein synthesis and decomposition in the body of exercise, and the mechanism of collective protein response to exercise stimulation has not been fully understood. Therefore, excessive application of protein kinetics in the study of metabolic reactions must be limited in research methods.

As a result of the limitation of research methods, the extra protein can promote the increase of the performance is still lack of effective argument, but it is undeniable that the positive role of complement proteins or amino acids for human body is obviously, athletes reasonable standard use of protein supplements should be the broad masses of sports nutrition researchers attention.

Delayed muscle soreness is common in athletes under excessive exercise pressure. Since athletic skeletal muscle microinjuries can affect athletes' athletic ability, interfere with athletes' psychological and level performance, and shorten the repair time of skeletal muscle microinjuries, they play a very important role in alleviating athletes' muscle pain and improving athletes' training effect. Reduce the negative effects of skeletal muscle microinjury. On the one hand, reduce sports training and competition at the physical level after delayed muscle soreness, so as to promote rapid recovery of the body. On the other hand, it is also possible to accelerate the repair of injury with reasonable intake of nutrition under the premise of not violating sports ethics. Supplements such as vitamins, protein, amino acids, unsaturated fatty acids and carbohydrates can be taken to meet athletes' needs to a certain extent. The use of supplements to quickly repair muscle damage has been the focus of many researchers, but the results have so far been limited. It is not difficult to find from

the research results at home and abroad that the prevention and treatment or improvement of delayed muscle pain is a worldwide problem in the field of sports medicine, and there is no authoritative repair method. In this study, on the basis of being open, from the perspective of nutritional intervention, by adding active peptide of micro damage effect, discusses the method of prevention and cure micro exercise-induced skeletal muscle damage, protect micro damage occurrence and promote the regeneration of the new type of nutrition enhancer to provide experimental basis, expect the proposed research methods and research results in our study can provide the public with the objective of supporting results.

2.4. Surface Skeletonization Algorithm Based on Fuzzy Distance Transformation

(1) Fuzzy distance transformation theory

Let Z^n denote the n-dimensional digital grid space, the digital object O is a fuzzy subset of Z^n , then O is an ordered pair set, which is defined as follows:

$$O = \{(p, \mu_o(p)) \mid p \in Z^n\} \quad (4)$$

Where p represents a point in the grid space, and $\mu_o : Z^n \rightarrow [0,1]$ represents the membership function of set O in Z^n . Let θ_o denote the support domain of O , then:

$$\theta_o = \{p \mid p \in Z^n, \mu_o(p) \neq 0\} \quad (5)$$

That is, θ_o represents the set of non-zero membership values in Z^n , which is the foreground object. On the contrary, $\bar{\theta}_o$ means the set of points with zero membership in Z^n , which is the background object. The length of two adjacent points p and q is defined as follows:

$$\frac{1}{2}(\mu_o(p) + \mu_o(q)) \times \|p - q\| \quad (6)$$

Among them $\|p - q\|$ represents the distance between p and q . Commonly used distances mainly include Euclidean distance, chessboard distance, and city block distance. Assuming that the coordinates of p and q are (P_1, P_2, \dots, P_n) and (q_1, q_2, \dots, q_n) , respectively, the definitions of the Euclidean distance, chessboard distance, and city block distance of p and q are as follows: (7), Formula (8) and Formula (9). Since the Euclidean distance can accurately reflect the true distance between two points in the grid space, the algorithm in this chapter will use the Euclidean distance to calculate.

$$\|p - q\| = \sqrt{(p_1 - q_1)^2 + (p_2 - q_2)^2 + \dots + (p_n - q_n)^2} \quad (7)$$

$$\|p - q\| = |p_1 - q_1| + |p_2 - q_2| + \dots + |p_n - q_n| \quad (8)$$

$$\|p - q\| = \max_{1 \leq i \leq n} \{p_i - q_i\} \quad (9)$$

Let p and q denote two points in Z^n , then the path

$\Pi = \{p_1, p_2, \dots, p_m \mid p_i \neq p_j, 1 \leq i \neq j \leq m\}$ from p to q is a sequence of points, in which any point

pair p_i and p_{i+1} ($1 \leq i < m$) are adjacent points. The length $\pi_o(\pi)$ of the path π is the sum of the lengths of adjacent points on the path π , then:

$$\Pi_o(\Pi) = \sum_{i=1}^{m-1} \frac{1}{2} (\mu_o(p_i) + \mu_o(p_{i+1})) \times \|p_i - p_{i+1}\| \quad (10)$$

Suppose there are multiple paths between p and q , and use $\Gamma(p, q)$ to denote the set of these paths, then there must be one path in $\Gamma(p, q)$ so that the length of the path between p and q is the smallest. Use $w_o(p, q)$ to represent the shortest path length from p to q , then:

$$w_o(p, q) = \min_{\Pi \in \Gamma(p, q)} \{\Pi_o(\Pi)\} \quad (11)$$

The blur distance of all points in θ_o is defined as 0, and the blur distance of point p in θ_o is defined as the shortest path length to θ_o , which is represented by $\Omega_o(p)$, then:

$$\Omega_o(p) = \min_{q \in \theta_o} \{w_o(p, q)\} \quad (12)$$

(2) Membership function

CT scanning is a non-invasive functional imaging technique in which iodine concentration and tissue density change linearly with time (1ml iodine increases the CT of 1ml tissue by 25Hu) and the obtained curve is called the time / density curve. Although there are series of other imaging techniques to evaluate tissue perfusion, CT imaging is characterized by short scanning time, high spatial resolution and simple and easy technology. While showing blood flow changes, it indirectly reflects the tissue vascular distribution and vascular physiology, and is relatively simple compared with the complex MR fusion model, which is an ideal technique for tissue perfusion evaluation. The mathematical models of CT are mainly divided into two categories, the non-deconvolution and deconvolution methods. Non-deconvolutional calculations often result in underestimated blood flow and high requirements for contrast agent injection rate and more difficult to operate.

CT perfusion imaging has been widely used in clinical practice, such as perfusion imaging of cerebral ischemic diseases, myocardial perfusion, pulmonary embolization, renal ischemic disease, and CT perfusion parameters of normal liver and cirrhosis. In the field of tumors, CT perfusion imaging can reflect microvascular changes in tumor angiogenesis, thus assessing tumor goodness, malignancy, stage, grade, and even observations of efficacy before and after treatment. It can be applicable to this study.

In digital fuzzy objects, the membership function can be regarded as a continuous gray-scale transformation function. Different from the binarization function,

For the fuzzy boundary that cannot be determined by the threshold, the fuzzy object describes the probability of belonging to the foreground object through the membership degree value.

Choosing an appropriate membership function is the key to extracting the foreground of fuzzy objects. Saha counts the gray histogram of the digital image, and defines the membership function according to the peak information of the histogram. The calculation formula of the membership function is as follows:

$$\mu_o(p) = \begin{cases} 0 & f(p) < \mu_M \\ \frac{f(p) - \mu_M}{\mu_F - \mu_M} & \mu_M \leq f(p) \leq \mu_F \\ 1 & \mu_F < f(p) \end{cases} \quad (13)$$

Where $f(p)$ represents the gray value of point p in the image, and μ_M is the average value of μ_B and μ_F . Use a smooth Gaussian function as the membership function, which is defined as follows:

$$\mu_o(p) = \begin{cases} G_{m_A, \sigma_A}(f(p)) & f(p) \leq m_A \\ 1 & m_A < f(p) \end{cases} \quad (14)$$

Among them, m_A and σ_A represent the average value and standard deviation of the gray scale respectively, and G is the Gaussian function.

LK Huang pointed out that the membership value of each former scenic spot in the image should not be less than 0.5. Therefore, this paper selects a smooth exponential function with base 2 as the membership function, as shown below:

$$\mu_o(p) = \begin{cases} 0 & f(p) < \mu_{TH} \\ \frac{f(p) - \mu_{FM}}{2\mu_{FM} - \mu_{TH}} & \mu_{TH} \leq f(p) \leq \mu_{FM} \\ 1 & \mu_{FM} < f(p) \end{cases} \quad (15)$$

Among them, μ_{TH} is the segmentation threshold of the grayscale image, and μ_{FM} is the average value of the foreground grayscale of the image specified by the threshold μ_{TH} . In this paper, the threshold algorithm based on fuzzy set theory proposed by LK Huang is used to calculate the segmentation threshold. The algorithm uses Shannon entropy to measure the ambiguity. For all possible thresholds, the smallest value of Shannon entropy is taken as the final segmentation threshold. The threshold calculated by this algorithm is slightly lower than the national value calculated by traditional Ostu and other algorithms, which can preserve more boundary information of the object.

3. Experimental Design

3.1. Experimental Subjects and Grouping

Dawley (SD) rats, License No: SCKK(Jing) 2016-0006. It was raised in the animal room of the clean IVC feeding system of Sports Nutrition Center of Institute of Sports Medicine, raised in cages (4 / cages), free water (sterile water) and feeding. The relative humidity in the animal room was about 60%, the room temperature was 25 ± 2 °C, indoor lighting automatic control system adjusted day and night, and the light and dark cycle was 12h(light illumination time 06:30-18:30).

A total of 54 SD male rats, 17 ± 3 weeks old and 320 ± 20 g weight, were selected from the animal experimental center of Our province for this study. After the completion of selection, the rats were first raised freely in cages and then screened in experiments. After screening, it was found that 6 rats were not suitable for experimental animals for other reasons, so they were excluded. A total of 48 rats were included in the animal experiment, and these rats were divided into the control group, the immediate centrifugal exercise group, the 24h group, and the 48h group. Regardless of weight

differences and other factors, the rats were still kept in cages before the experiment was carried out. The temperature was controlled at $23 \pm 3^{\circ}\text{C}$, and the environmental relative humidity was 50-65%. The living environment of the rats was controlled by daylight rhythm lamps day and night. All rats were free to eat and rest freely. Setting the supplementation and placebo group, during the validation of the ethics committee.

3.2. Animal Movement Model

The rats in the control group did not take any intervention measures and were still in the free feeding mode. Rats in the simulated centrifugal exercise group, including the immediate group, the 24h group and the 48h group, were subjected to intermittent treadmill test. The experimental speed of the treadmill was set at 15m/min, and the slope of the treadmill was set at 17° . The rats were set to take a rest once every 5 minutes after performing treadmill training, and each rest time was set at 2min, and the total daily exercise time was set at 150min. In order to ensure that the energy consumption of the rat body is not stimulated by external factors to the maximum extent, we decided to give up the use of electrical stimulation and adopt the indirect contact mode of artificial driving or sound stimulation. Rats in the exercise group were perfused with 15% soy protein isolate after exercise. At the end of the experimental period, rats were anesthetized with 20% urrtan peritoneal anesthesia immediately after the end of the experiment, 24h and 48h, respectively, and the specimens were quickly collected and prepared. The whole process strictly implements the regulations of the animal experiment ethics Committee and gives the experimental animals due ethical care. Among them, rats in the control group were not infused with soy protein isolate, but given the same amount of pure water by gavage, and were also raised separately in the metabolic cage.

3.3. Test Indexes and Test Methods

After 0.1g/ml samples are taken and mixed with concentrated sulfuric acid, they are placed in a Kjeldner flask, heated and digested on an adjustable electric heating plate, cooled and diluted to 50mL, and 3ml of the diluted digestive juice is taken and distilled in a Kjeldner nitrogen distillation unit. Distillation will continue until the indicator is mixed in the bottle and the color changes from red to green. Distillation will continue for 2min, and then titrate with standard hydrochloric acid. After waiting for the terminal color to change to light green, the amount of hydrochloric acid will be recorded.

The mouse was prepared into 5% homogenate with 50mm mannitol solution at 4°C . The homogenate was 100 L and the protein content was measured according to Bradford method. Add anhydrous calcium chloride to the rest of the homogenate, stir and let stand for 10 minutes, centrifuge for 10 minutes, and leave the supernatant. The precipitation was centrifuged again with tris-mannitol solution, leaving the supernatant. The anteroposterior supernatant was used to determine the activity of aminopeptidase. The supernatant (20 μl) was added with 0.5mML bright-aminoyl $-\beta$, 50mM phosphate buffer and 0.38ml distilled water, washed for 60min at 37°C , and the reaction was stopped after adding 0.2mol/ L acetate buffer. The Anti-TLR4 antibody dilution ratio was 1:1000, Anti-MyD88 anti body dilution ratio 1:2000, Anti-Bax antibody dilution ratio 1:500.

3.4. Serum CK Isoenzyme Test

50ul serum samples were taken from each group of rats. After being shaken well, 10UL activated samples were added and placed in a humectant for 10min for electrophoresis. Electrophoretic developer was prepared simultaneously: the main components were matrix solution, ISO-CK dry powder matrix and 7.5ml developer solution. After the electrophoresis, the sampling comb was removed and the sampling template was placed. The sealing solution was removed at 37 °C, and the sampling template was removed and dried. After drying, take out the sample film for scanning.

3.5. Determination of Gastrocnemius Nebulin Content

After the protein concentration of the skeletal muscle samples to be measured was adjusted, the 100x130mm vertical plate electrophoresis tank was used for electrophoresis. The separation gel concentration was set at 8%, the concentration of concentrated gel was 5%, and the sample amount of protein per well was 60ug. When the sample passed through the concentrated gel, the voltage was stable at 48V, and the electrophoresis time was controlled within 5 hours. In particular, the normative operation of stopping the electrophoresis with bromophenol blue swimming to the bottom of the gel was completed. After the electrophoresis, the PVDF membrane was placed in the PBST solution with 3% content for storage. To ensure the smooth operation of the membrane, the β -actin sample was added every 10 minutes. After 3 cycles of the sample, the film was exposed by chemical method and displayed in the protein band.

3.6. Test Calpain-1 and Calpain-2 Gene Expression

Total RNA was extracted from gastrocnemius muscle tissue according to the operating instructions. To ensure the integrity of RNA, THE OD value of RNA samples was measured by ultraviolet spectrophotometer. The extracted TOTAL RNA was reverse-transcribed into cDNA by two-step method, and the amplification reaction was projected on the MX350PCR System with fluorescence quantification. The primers and probes of Calpain-1 and Calpain-2 were Taqman MGB probes.

3.7. Mathematical Statistics

All experimental data were expressed as mean \pm standard deviation ($\bar{x} \pm s$). SPSS 23.0 was selected as the software platform for factor analysis, and the significance level was $P < 0.05$.

4. Experimental Results and Analysis

4.1. Possible Mechanism of Exercise-Induced Skeletal Muscle Micro-Injury and Repair

The main observations are the structure of skeletal muscle tissue, including the morphology of epimuscular membrane, nucleus, muscle fiber, interstitial small blood vessels, and inflammatory cells. The main manifestations of the morphological changes of skeletal muscle tissue under light microscope are: 1) swelling of muscle fibers; 2) uneven distribution of nuclei and nuclear aggregation; 3) granular degeneration, vacuolar degeneration, and discoid degeneration of muscle fibers; 4) Phagocytosis of muscle fibers, myolysis, and focal necrosis, scarring, etc.; 5) interstitial edema, inflammatory cell infiltration, small blood vessel dilation, intravascular thrombosis, venous

congestion, and small arterial congestion.

In the quiet group (normal), the muscle fibers of the rats were tightly arranged. Obvious muscle stripes were seen on the longitudinal section, and the fibers on the transverse section were polygonal and uniform in size. The nuclei are evenly distributed under the muscle membrane around the fibers, without hyperplasia, swelling or pyknosis. The morphology of the blood vessels between the tissues was normal without rupture. No fibrous hyperplasia was seen in the epimuscular membrane. After eccentric exercise, the morphology and structure of skeletal muscle of rats in each group changed to different degrees. The results of the changes are shown in Table 1, and the changes are shown in Figure 5, and this change after exercise has obvious temporal characteristics. For example, the initial stage is characterized by changes in interstitial blood vessels and inflammatory cell infiltration, followed by muscle cell swelling. , Muscle fiber degeneration and even necrosis; after a number of independent samples of non-parametric tests (Kruskal-Wallis H), it was found that the differences in the changes in the microstructure immediately after exercise were not significant at the 0.05 level ($P > 0.05$ A \rightarrow B1 inflammation Except for cell infiltration and changes in interstitial small blood vessels), the difference in changes from immediately after exercise to later time points is significant at the 0.05 level ($P < 0.05$ B1 \rightarrow B2 B1 \rightarrow B3 B1 \rightarrow B4), but exercise The differences in the changes from the last 24 hours to the 72 hours are not significant at the 0.05 level ($P > 0.05$ B2 \rightarrow B3 B2 \rightarrow B4), and the changes from 48 hours to 72 hours after exercise except for the difference in myolysis Except for the significance at the 0.05 level, although the others are not significant, the P value is reduced. The P value is shown in Figure 4. These results indicate that the effect of eccentric motion on the fine structure of skeletal muscle is delayed. The changes in the morphological structure of this organization are the most serious within 24-48 hours after exercise.

Table 1. Changes in the microstructure of skeletal muscle after eccentric exercise (%)

Changes in each group and their rate of change	Quiet group (A)	Immediately after exercise(B1)	After exercise 24Hr(B2)	After exercise 48Hr (B3)	After exercise 72Hr (B4)
Myocyte swelling	0	0	6.85 \pm 1.50	6.30 \pm 1.75	4.20 \pm 0.70
Muscle fiber degeneration	0	0	5.88 \pm 1.03	6.38 \pm 1.18	4.00 \pm 0.95
Inflammatory cell infiltration	0	0.77 \pm 0.11	3.85 \pm 0.85	5.33 \pm 1.03	4.35 \pm 0.63
Changes in interstitial small blood vessels	0	0.74 \pm 0.09	3.65 \pm 0.58	4.65 \pm 0.73	3.40 \pm 0.70
Myolysis	0	0	3.88 \pm 0.73	4.48 \pm 0.48	2.98 \pm 0.53

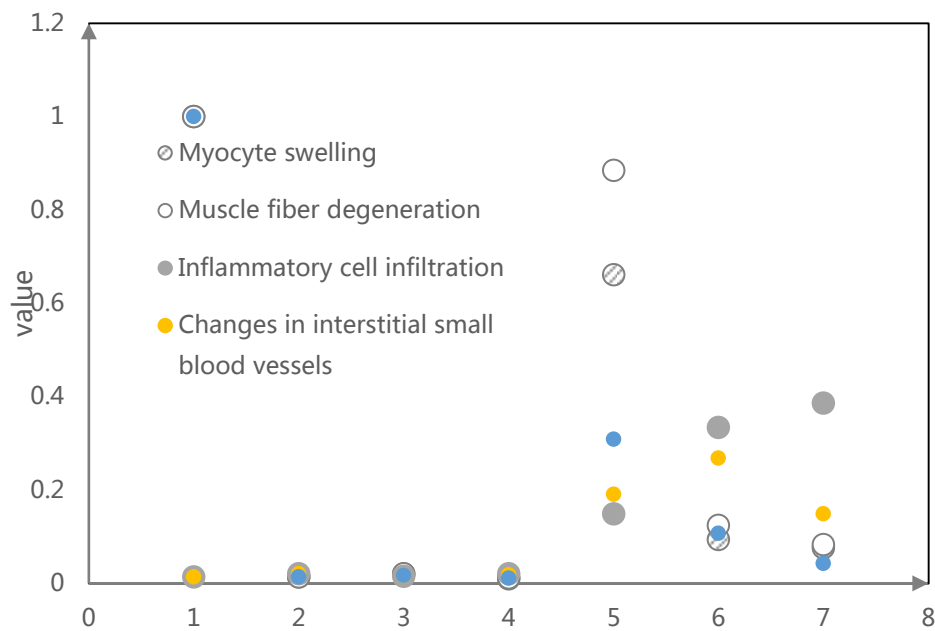


Figure 4. P value of various microstructure changes of skeletal muscle after eccentric exercise (Kruskal-Wallis H test)

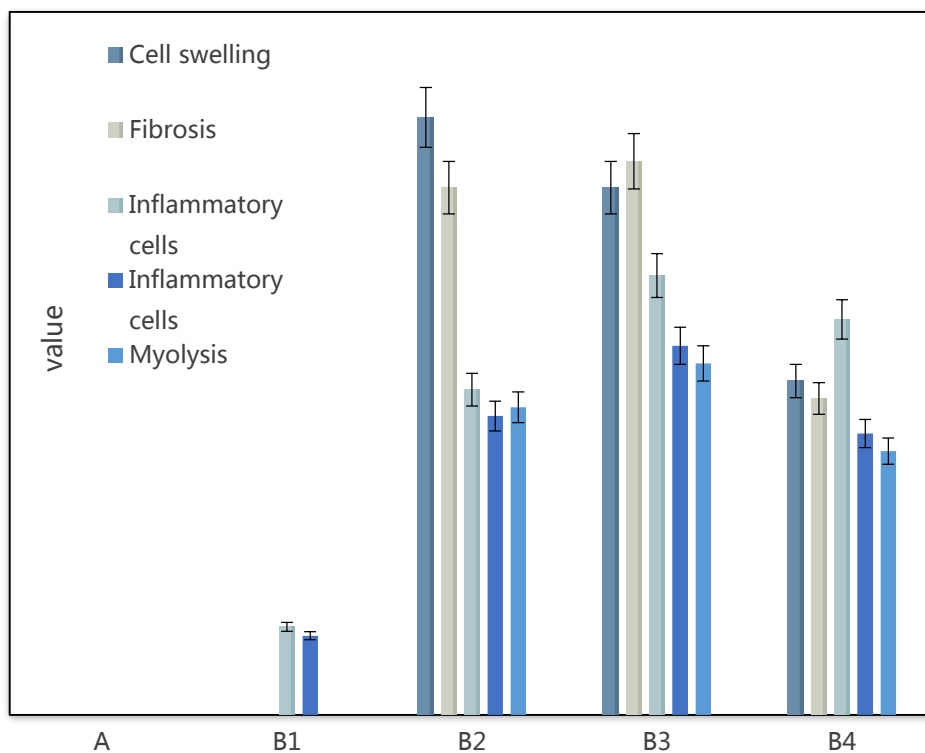


Figure 5. Changes in the microstructure of skeletal muscle after eccentric exercise

(2) Observation of cytoskeletal protein expression of skeletal muscle cells in rats after a one-time eccentric exercise

Both desmin and vimentin in the muscle tissue of normal rats are distributed in a net shape; desmin and vimentin are both expressed after exercise. The boundary of desmin-positive muscle cells is clear and flaky, and the boundary of vimentin-positive muscle cells is blurred, Distributed in a spot-like shape. The percentage of destained cells when desmin is at rest is zero (its immune response score is the highest), and different degrees of anti-desmin staining and destaining occur at different time periods after exercise, and the percentage of destained cells increases to varying degrees (Immune response score decreased), with the greatest degree of change in 24 hours. The change (destaining) of anti-desmin antibody staining in skeletal muscle cells is a reflection of the dynamic changes in the assembly and disassembly of desmin, and is one of the manifestations of damaged cells. After the non-parametric test of multiple independent samples (Kruskal-Wallis H), it was found that the changes in cytoskeleton protein expression indicators immediately after exercise were significant at the 0.05 level ($P < 0.05$ A → B1 Desmin immune response Except for scores), the difference in changes from immediately after exercise to 72 hours is significant at the 0.05 level ($P < 0.05$ B1 → B2 B1 → B3 B1 → B4, except for the immune response score of desmin), but exercise The difference in the changes from the last 24 hours to 72 hours was not significant at the 0.05 level ($P > 0.05$ B2 → B4). Therefore, the experimental results of this study indicate that desmin in the skeletal muscle of rats after an eccentric exercise The expression has decreased, most notably 24 hours after exercise. Desmin expression began to increase after 48 hours, and it could not be restored after 72 hours, as shown in Table 2 and Figure 6.

Table 2. Changes in the expression of skeletal myosin after eccentric exercise

Group	Immune Response Score (IRS)	Negative cell%
Quiet (A)	2320.25 ± 386.75	0
Immediately after exercise (B1)	1790.50 ± 273.50	6.09 ± 2.19
24 hours after exercise (B2)	1275.25 ± 270.25	18.43 ± 3.49
48 hours after exercise (B3)	1302.75 ± 246.75	15.96 ± 2.31
72 hours after exercise (B4)	1421.25 ± 245.25	8.88 ± 2.01

Test Statistics a, b: $P = 0.029 < 0.05$ (IRS, A → B4), $P = 0.01 < 0.05$ (NC%, B1 → B4)

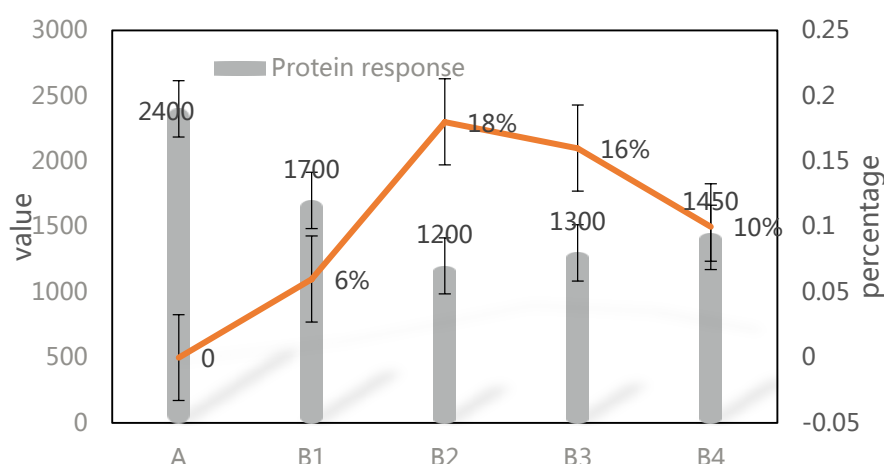


Figure 6. Changes in the scores of rat skeletal myosin immune response and the percentage of de-stained cells

4.2. Changes of Serum Activity and Gastrocnemius mRNA Expression

The changes of serum activity and gastrocnemius mRNA expression were shown in Table 3 and Figure 7. As can be seen from the chart, the activity of CK-MM in the immediate group increased to the highest value after exercise, which was significantly higher than that in the control group. The activity of serum CKMM in the exercise group was significantly lower than that in the immediate group at 24h and 48h. In terms of Calpain-1 and Calpain-2 gene expression, the expression of Calpain-1 mRNA in the immediate exercise group was significantly decreased compared with that in the control group, while no significant abnormalities were found in the other groups. In addition, Calpain-1 mRNA expression reached its lowest level 24h after exercise, and returned to the normal gene expression level about 48h after exercise.

Table 3. Changes of serum activity and gastrocnemius mRNA expression

Group	Control group	Immediate group	24h group	48h group
Serum CK - MM (U/L)	60.55±21.57	104.44±47.92	66.40±13.00	52.80±12.55
Gastrocnemius calpain-1 mRNA	1.00±0.00	0.44±0.12	0.13±0.02	0.40±0.16
Gastrocnemius calpain-1 mRNA	1.00±0.00	0.47±0.17	0.24±0.19	0.39±0.14

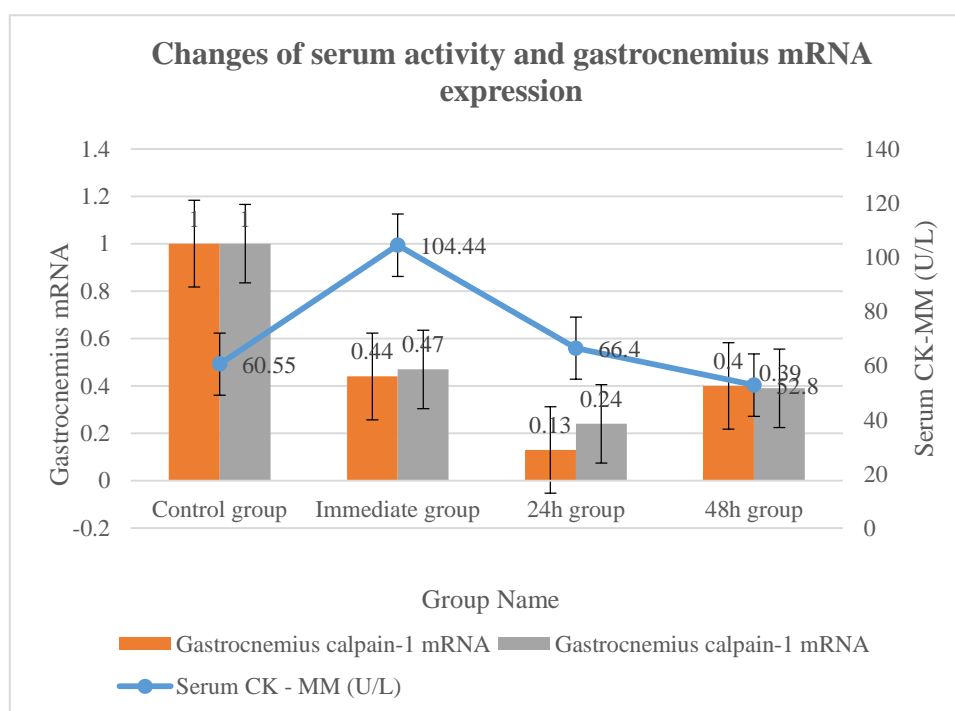


Figure 7. Changes in serum activity and gastrocnemius mRNA expression

4.3. Changes in Skeletal Muscle and Gastrocnemius Content

The changes of skeletal muscle and gastrocnemius were shown in Figure 8. Can be found from the figure, Nebulin quantity of protein expression in each time after motion nodes were higher than the control group. In the comparison of 24h and 48h time nodes, 24h decreased slightly, but reached

the peak value at 48h after exercise. Nebulin protein expression pyrolysis products of the quantity change trend is flat, and on the pyrolysis product value is high, the more protein degradation characteristics. Can visually see from the graph, Nebulin protein expression pyrolysis product quantity for peak in immediately after exercise, exercise during 24 h, 48 hours is slightly higher, but not obvious. After exercise, the expression of Ttin protein in gastrocnemius showed a rapid decrease, and the rate of decrease was faster, and it was restored to the normal level within only 24h.

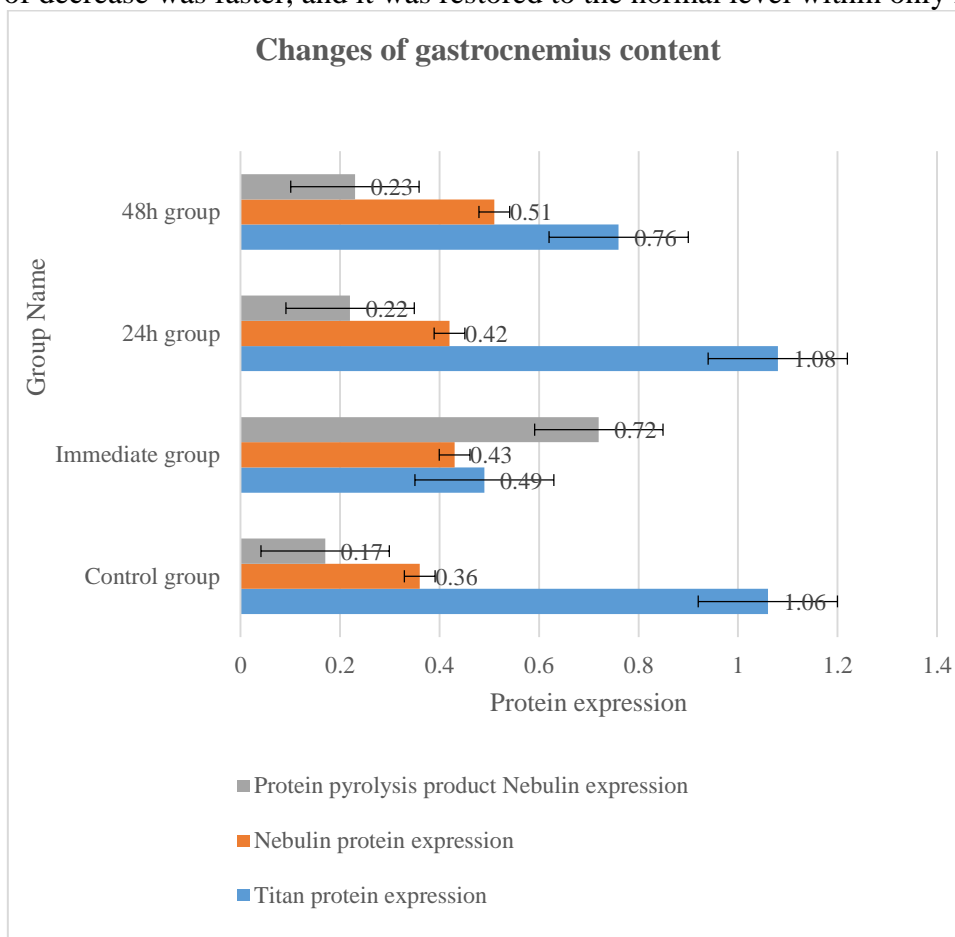


Figure 8. Changes in skeletal muscle and gastrocnemius content

4.4. Blood Biochemical Indexes

The results of blood biochemical indicators are shown in Table 4 and Figure 9. As can be seen from the data in the chart, compared with the control group, il-6 index of each exercise group showed a trend of gradually increasing at each time node after exercise, among which the increase at 24 hours after exercise was the most obvious and the level at 48 hours after exercise reached the highest level, which was significantly higher than that of the control group. In terms of serum T-AOC changes, the immediate group, 24-hour group and 48-hour group of the exercise rats were significantly higher than the control group, reaching the peak value at 48h. In terms of the changes of serum SOD, SOD activity in the immediate group, 24h group and 48h group was significantly lower than that in the control group. Although the activity of 48h gradually increased, there was no significant difference among the three groups. In terms of the changes of serum SOD, the immediate group, the 24h group and the 48h group in the exercise group were significantly higher

than the control group, and there was no significant difference between the three exercise groups. In terms of serum LDH changes, there was no significant difference in serum LDH activity between the exercise group and the control group at each time node, but there was a significant difference between the exercise groups, which showed that the LDH activity of the rats in the immediate group increased significantly and was at the peak value, while the LDH activity of the rats in the immediate group decreased significantly at 24h and 48h.

Table 4. Results of blood biochemical indexes

Group	Control group	Immediate group	24h group	48h group
IL-6(pg/ml)	570±126	590±160	760±240	824±259
T-AOC(U/ml)	9.9±1.1	12.5±2.06	13.7±1.20	17.9±3.35
SOD(U/ml)	116.2±20.1	87.5±16.6	92.3±9.50	85.3±14.2
MDA(U/ml)	5.3±1.49	6.2±2.23	5.8±1.56	5.4±1.6
LDH(U/ml)	532.6±94.0	1127.4±213.03	1058.2±259.1	1736.5±212.4

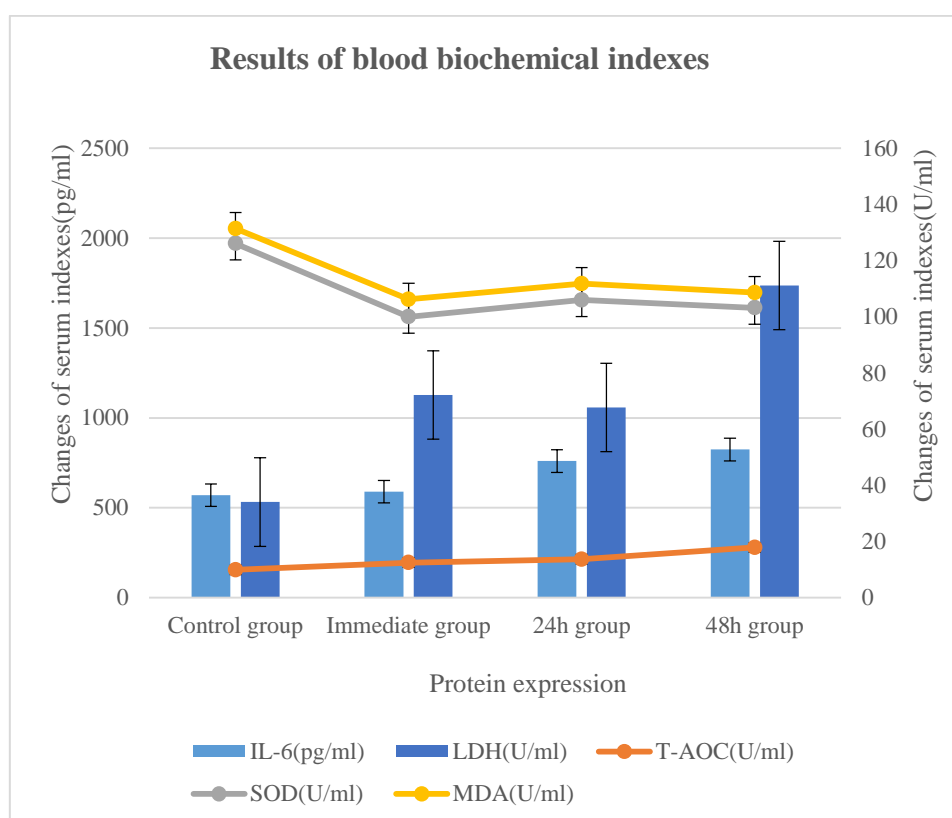


Figure 9. Results of blood biochemical indexes

4.5. Effects of Supplementary Protein on the Expression Changes of Skeletal Muscle Cells after Centrifugal Exercise

Supplementing soy protein within 1 hour after exercise has a certain degree of inhibitory effect on the decrease of desmin expression in skeletal muscle caused by eccentric exercise. At any time after exercise, the phenomenon of skeletal muscle anti-desmin staining and de-staining will be

removed. The percentage of stained cells decreased by 38.42%, 29.84%, 40.60% and 30.18% immediately after exercise, 24 hours, 48 hours, and 72 hours, respectively; Decreased expression of desmin in skeletal muscle has a very good inhibitory effect. At any time after exercise, the phenomenon of skeletal muscle anti-desmin staining and de-staining, that is, the percentage of de-stained cells, is significantly reduced. Immediately after exercise, 24 hours, At 48 hours and 72 hours, there were 69.13%, 71.89%, 72.12%, and 58.56% lower than the corresponding water supplement. It shows that peptide supplementation has a better inhibitory effect on the decrease of skeletal myosin expression caused by exercise than protein supplementation, and it has a better promotion effect on its recovery after exercise. The statistical results and changes are shown in Figure 10 respectively.

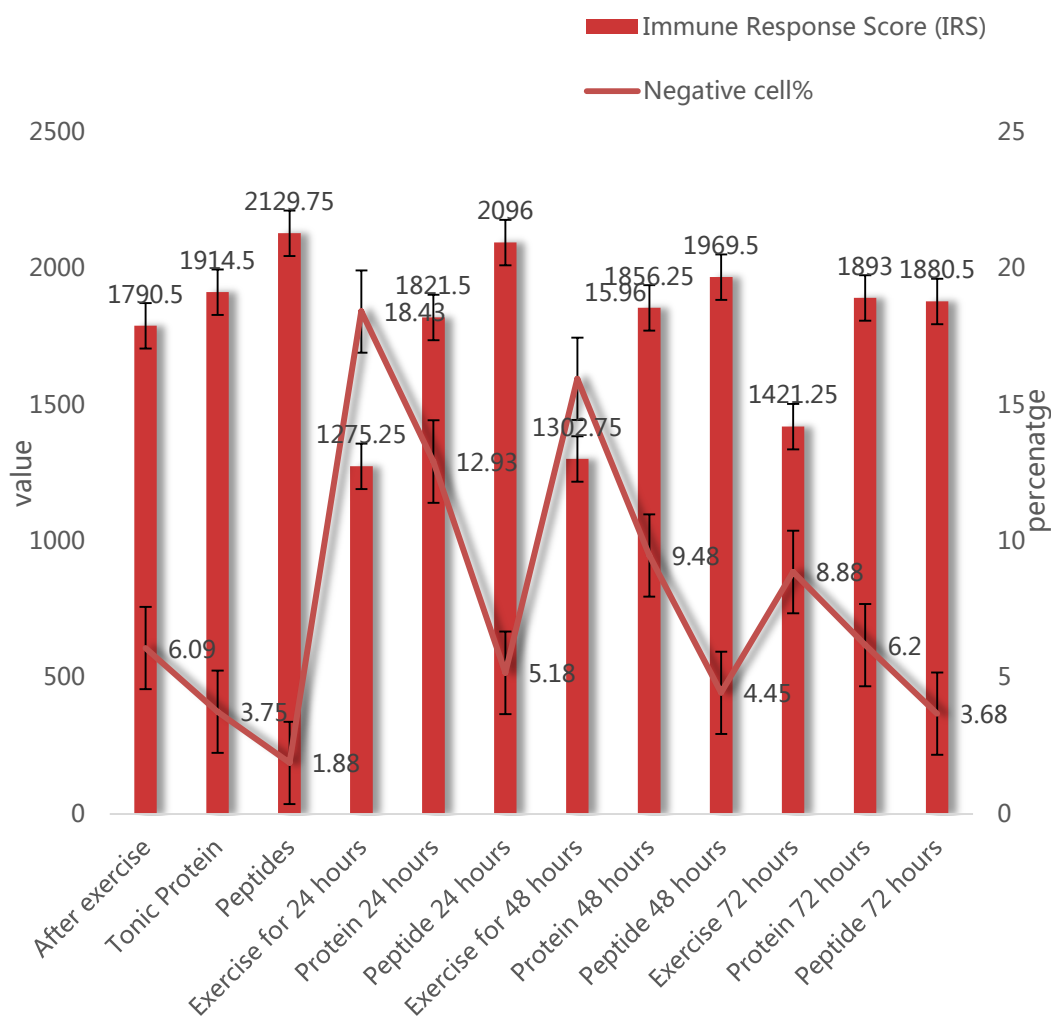


Figure 10. The effect of soy protein and soybean peptide supplementation on the expression of skeletal myosin after eccentric exercise

The influence of supplementary protein on the expression of skeletal muscle protein in rats after centrifugal exercise is shown in Table 5 and Figure 11. It can be seen from the figure that timely

supplementation of soy protein after exercise has a certain inhibitory effect on skeletal muscle structure damage caused by excessive exercise, and it can act on skeletal muscle anti-protein at any time period, resulting in a decrease in the percentage of destined cells. Within the group compared with control group, the movement of the immediate group, 24h, 48h group hydrating rate of supply and demand fell by 32.53%, 27.32% and 24.26%, respectively, in a timely manner after the motion complement soybean polypeptide and protein expression in skeletal muscle drops with ideal inhibitory effect, after the movement of any period of time could make the phenomenon of skeletal muscle protein staining of the cell percentage significantly lower, also shows that compared with filling the repair protein peptide, protein expression reduction of skeletal muscle of movement is even more significant, but also more conducive to restore their physical condition after a sports injury.

Table 5. Effects of supplementary protein on the expression of skeletal muscle protein in rats after centrifugal exercise

Group	Immune response score	Destained cells %	Positive cells %
Control group	2312.24±372.53	0	0
Immediate group	1793.32±217.37	6.37±1.24	0.17±0.08
24h group	1916.31±225.76	3.64±0.61	0.37±0.14
48h group	2127.33±427.13	1.84±0.55	0.76±0.25

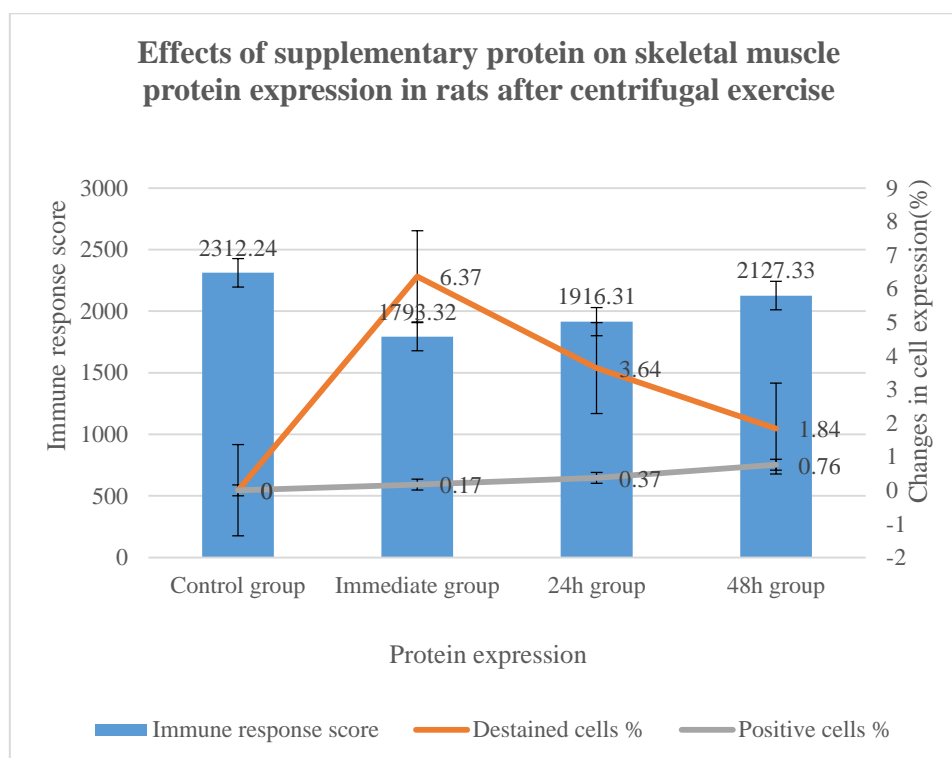


Figure 11. Effects of supplementary protein on changes in skeletal muscle protein expression in rats after centrifugal exercise

After exercise, the supplementation of soy protein had a good inhibitory effect on the expression

of vimentin in skeletal muscle induced by centrifugal exercise. Anti-vimentin would increase the function score of the immune system at any time after exercise, while the corresponding hydration demand was relatively decreased. In this study, compared with the control group, involved in the centrifugal movement immediate group, 24 h, 48 h group of filling water demand has fallen by 55.21%, 28.39% and 6.2%, respectively, after the movement added soybean polypeptide skeletal muscle microstructure damage caused by eccentric exercise has better inhibition effect, and the recovery after exercise has better promoting effect.

5. Possible Relationship between Protein Nutrition Supplement and Exercise-induced Skeletal Muscle Microinjury and Repair

The body is more likely to cause changes in skeletal muscle microstructure after intense and asymmetrical motion, especially after centrifugal motion, which has been confirmed by numerous studies, and the experimental results in this study also confirm this fact again. We found that the histological morphological and structural changes and ultrastructural changes of skeletal muscle were almost inevitable after the occurrence of high intensity centrifugal exercise, and had the delayed characteristics of muscle dominant injury. Results in the immediate group after the end of the centrifugal exercise showed that the initial stage was characterized by visible muscle cell swelling, followed by vascular changes and inflammatory cell infiltration, and even muscle fiber degeneration and necrosis. The histological morphological changes observed in sections were most obvious 24h after exercise, and the peak value of ultrastructural changes was also at this moment. It was found that the histological changes and ultrastructural changes of skeletal muscle were significantly reduced after centrifugal exercise. At 24h after exercise, skeletal muscle microstructure damage reached its peak. At 48h after the exercise, the repair of skeletal muscle microstructure injury was basically completed. This suggests that protein nutrition supplementation has a good promoting effect on the repair of post-exercise micro-injury. We speculate that the possible reason is that the active peptide can increase the storage of glutamine in skeletal muscle, increase the synthesis of protein, and prevent the degradation of muscle protein. Or it could be that soy protein itself is a powerful antioxidant that protects against free radicals attacking cell membranes.

In this study, compared with the control group, involved in the centrifugal movement immediate group, 24 h, 48 h group of filling water demand has fallen by 55.21%, 28.39% and 6.2%, respectively, after the movement added soybean polypeptide skeletal muscle microstructure damage caused by eccentric exercise has better inhibition effect. As for the digestion, absorption and utilization of proteins, it has been believed that the body relies on the intestinal absorption of amino acids to obtain the necessary nitrogen for protein synthesis. But the latest research suggests that small titanium molecules may be absorbed directly by the gut to make small peptides. The active peptide molecule can not only provide abundant nitrogen source for the body, but also have some biological functions necessary for the body operation, such as promoting mineral element absorption, anti-tumor, anti-oxidation, immune regulation and hormone action.

Amino acid molecules and small peptide molecules are two transport systems with different mechanisms of action and specific characteristics. Because of their mutual exclusion, the molecules that transport the peptides are often unable to transport the amino acids, and likewise, the molecules that transport the amino acids are unable to transport the peptides. The protein was hydrolyzed by enzyme in digestive tract to form 30% oligopeptide containing several amino acid residues and 70% free amino acid. Free amino acids can be broken down by aminopeptidase into small peptides

directly into the blood to promote the rapid absorption of small peptide fractions.

The importance of protein for exercise is self-evident. In fact, as early as the 19th century, biologists proposed that the amino acids produced by protein degradation could be used as the main fuel for exercise and maintain long-term muscle movement. However, because of the immature experimental environment, this idea could not be verified effectively. After the 1980s, due to the rapid development of genetic and biological detection conditions, biological detection techniques and methods are enough to carry out the study of the role of proteins in movement, so that people gradually realized that the role of proteins in human movement is far more than originally thought. People began to realize that proteins can be quickly absorbed and efficiently used in sports in the form of small peptides. Therefore, direct supplementation of active peptides began to circulate among special groups such as athletes in games, and their efficacy was verified.

Protein can stimulate muscle sugar and promote the repair and regeneration of skeletal muscle after exercise. In the process of exercise, when glycogen reserves in the body are sufficient, supplementing active peptide can not only avoid consuming high-protein food, but also can damage the body's health, etc., so as to reduce the intestinal digestion burden, improve the absorption efficiency of small peptide, and create a hormone environment conducive to anabolic metabolism for skeletal muscle. Adequate protein supply, coupled with scientific training, can promote the body's muscle growth, promote the body's positive nitrogen balance, increase muscle strength. During exercise, if the muscle glycogen in the body is almost exhausted, protein may increase by more than 10%. When the muscle glycogen in the body is fully stored, protein supply accounts for about 5% of energy needs. At the same time, exercise also stimulates active skeletal muscle protein metabolism. Of course, these also depend on the specific type of exercise, the intensity of the exercise and the athlete's original physical state of a complex set of factors. In general, the catabolism of skeletal muscle protein is greater than that of anabolism in the period after high-intensity exercise, and the net degradation of contractin directly causes changes in skeletal muscle ultrastructure, which we speculate is due to delayed muscle pain. In the recovery stage of sports injury, skeletal muscle protein degradation is gradually inhibited, and skeletal muscle protein anabolism is increased for repairing and rebuilding skeletal muscle. When the degradation rate exceeds the anabolic rate, the protein will enter the body quickly in the first time to be quickly utilized by the body, enhance muscle protein, reduce inflammation caused by chronic muscle injury, and alleviate DOMS.

6. Conclusion

After the non-parametric test of multiple independent samples (Kruskal-Wallis H), it was found that the changes in cytoskeleton protein expression indicators immediately after exercise were significant at the 0.05 level ($P < 0.05$ A→B1 Desmin immune response Except for scores), the difference in changes from immediately after exercise to 72 hours is significant at the 0.05 level ($P < 0.05$ B1→B2 B1→B3 B1→B4, except for the immune response score of desmin). From the perspective of nutritional intervention, this study explored the prevention and treatment of exercise-induced skeletal muscle microdamage by supplementing the role of active peptide microdamage. Research for eccentric exercise rats model to simulate the basketball movement, the observation group respectively in the rat skeletal muscle after eccentric exercise serum CK-MM, Calpain, Titin and Nebulin of the gastrocnemius muscle protein expression. Results The main conclusions are as follows:

(1) Skeletal muscle has a buffering adaptation process to certain intensity of exercise. When the

intensity of exercise exceeds the limit that the body can bear, skeletal muscle will inevitably undergo structural changes and develop delayed sexually transmitted diseases, with muscle soreness as the main dominant symptom.

(2) After strenuous exercise, skeletal muscle will be damaged and blood indicators will change accordingly. Protein supplementation can enhance muscle protein synthesis and reduce protein degradation, so as to promote rapid recovery of skeletal muscle microstructure damage.

In the later work, it is a complex problem to promote body repair through tissue engineering technology, considering not only the activity of the transplanted cells and the regulation of in vivo differentiation, but also the choice of cell dilutions and the difference between the injection site when transplantation. After these problems are solved, the effect of using cell transplantation technology to treat skeletal muscle injury will be greatly improved.

Funding

This article is not supported by any foundation.

Data Availability

Data sharing is not applicable to this article as no new data were created or analysed in this study.

Conflict of Interest

The author states that this article has no conflict of interest.

References

- [1]Luo, A., Tang, C. L., Huang, S. Q. (2018). *Changes in Expression of Autophagy-related Factors during Acute Contusion Repair of Skeletal Muscle*, *Chinese Journal of Applied Physiology*, 34(2), pp. 97-101. DOI:10.12047/j.cjap.5647.2018.024
- [2]Hu, M. , Zhong, Y. , Xie, S. , Lv, H. , & Lv, Z. . (2021) *Fuzzy System Based Medical Image Processing for Brain Disease Prediction*. *Frontiers in Neuroscience*, 965. DOI:10.3389/fnins.2021.714318
- [3]Mohammadkhah, M., Simms, C. K., and Murphy, P. (2017). *Visualisation of Collagen in Fixed Skeletal Muscle Tissue using Fluorescently Tagged Collagen Binding Protein CNA35*, *Journal of the Mechanical Behavior of Biomedical Materials*, 66(1), pp. 37-44. DOI:10.1016/j.jmbbm.2016.10.022
- [4]Zhang, S. F. , Zhang, Y. , Li, B.(2018). *Physical Inactivity Induces the Atrophy of Skeletal Muscle of Rats through Activating AMPK/FoxO3 Signal Pathway*, *Eur Rev Med Pharmacol*, 22(1), pp. 199-209. DOI:10.26355/eurrev-201801-141
- [5]Górska, Magdalena, Wojtysiak D. (2017). *Pathological Changes in the Microstructure of Pale, Soft, Exudative (PSE) and Normal Turkey Breast Muscle*, *Folia Biologica*, 65(3), pp. 149-154. DOI:10.3409/fb65_3.149
- [6]Kochová, Petra, Hympanová, Lucie, Rynkevic R. (2016). *The Histological Microstructure and in Vitro Mechanical Properties of Pregnant and Postmenopausal Ewe Perineal Body*, *Menopause*, 26(11), pp. 1289-1301. DOI:10.1097/GME.0000000000001395
- [7]Xiao, F., & Ding, W. (2019) *Divergence Measure of Pythagorean Fuzzy Sets and Its Application*

- in *Medical Diagnosis, Applied Soft Computing*, 79, pp. 254-267. DOI:10.1016/j.asoc.2019.03.043
- [8]Zhou, S., and Tan, B. *Electrocardiogram soft computing using hybrid deep learning CNN-ELM. Applied Soft Computing Journal*, Volume 86, 2020, 105778. DOI:10.1016/j.asoc.2019.105778
- [9]Rehmann R, Schlaffke L, Vorgerd M. (2016). *FV 9. Diffusion Tensor Imaging in Neuromuscular Diseases - A Novel Method for Quantification of Muscle Degeneration in Myopathy Patients, Clinical Neurophysiology*, 127(9), pp. e214-e215. DOI:10.1016/j.clinph.2016.05.026
- [10]Shankar, K., Zhang, Y., Liu, Y., Wu, L., & Chen, C. H. (2020). *Hyperparameter tuning deep learning for diabetic retinopathy fundus image classification. IEEE Access*, PP (99), 1-1. DOI:10.1109/ACCESS.2020.3005152
- [11]Zanella S, Buccelletti F, Franceschi F. (2018). *Transnasal Sphenopalatine Ganglion Blockade for Acute Facial Pain: A Prospective Randomized Case-control Study, Eur Rev Med Pharmacol*, 22(1), pp. 210-216.
- [12]Zhang D, Tan Q, Tang S. (2016). *Evaluation of an Optimizing Protocol for Fabricating A Scaffold Derived from Porcine Skeletal Muscle Extracellular Matrix, Chinese Journal of Reparative & Reconstructive Surgery*, 30(10), pp. 1282-1289.
- [13]Y. Jiang, H. Song, R. Wang, M. Gu, J. Sun and L. Sha, (2017) *Data-Centered Runtime Verification of Wireless Medical Cyber-Physical System, in IEEE Transactions on Industrial Informatics*, 13(4), pp. 1900-1909. DOI:10.1109/TII.2016.2573762
- [14]Duan R Y, Huang M Y. (2016). *The Influence of Low-dose Cadmium on the Laryngeal Microstructure and Ultrastructure of Pelophylax Nigromaculata, Environmental Ence & Pollution Research*, 23(17), pp. 17322-17331. DOI:10.1007/s11356-016-6942-4
- [15]Naik A, Griffin M, Szarko M. (2020). *Optimizing the Decellularization Process of an Upper Limb Skeletal Muscle; Implications for Muscle Tissue Engineering, Artificial Organs*, 44(2), pp. 178-183. DOI:10.1111/aor.13575
- [16]Hrebikova H, Beznoska P, Bezrouk A. (2017). *Decellularized Skeletal Muscle: A Promising Biologic Scaffold for Tissue Engineering, Journal of Biomaterials and Tissue Engineering*, 7(6), pp. 491-498. DOI:info:doi/10.1166/jbt.2017.1588
- [17]Kang Y S, Kim C H, Kim J S. (2017). *The Effects of Downhill and Uphill Exercise Training on Osteogenesis-related Factors in Ovariectomy-induced Bone Loss, J Exerc Nutrition Biochem*, 21(3), pp. 1-10. DOI:10.20463/jenb.2017.0010